PHOTOMASK

BACUS—The international technical group of SPIE dedicated to the advancement of photomask technology.

Photronics Awards for Best Student Oral Finalist - PUV20

Picometer sensitivity metrology for EUV absorber phase

Stuart Sherwin, Laura Waller, and **Andrew Neureuther,** University of California Berkeley, Department of Electrical Engineering and Computer Science, Berkeley, USA

Isvar Cordova, Ryan Miyakawa, Markus Benk, and **Patrick Naulleau,** Center for X-Ray Optics, Lawrence Berkeley National Laboratory, Berkeley, USA

ABSTRACT

With growing interest in EUV attenuated phase shift masks due to their superior image quality for applications such as dense contact and pillar arrays, it is becoming critical to model, measure, and monitor the relative intensity and phase of multilayer and absorber reflections. We present a solution based on physical modeling of reflectometry data, which is capable of achieving single picometer phase precision. During repeated reflectometry measurements we observed a systematic change in absorber reflectivity which we attribute to the growth of a carbon film from 44-156pm, causing a change in the relative phase of 0.3°. This represents sensitivity to changes in the average film thickness to well below one atomic monolayer. After separating out systematic drift from random noise, we estimate our precision to be 3σ = 0.1°, corresponding to 3-4pm.

1. Introduction

In recent years interest in EUV attenuated phase shift masks (aPSMs) has increased, particularly for small-pitch dense patterns.[1] A traditional absorber cannot create a high contrast image without substantial bias due to the relative imbalance of the 0-order and scattered waves. An aPSM on the other hand uses destructive interference between the pattern and the background thus reducing the power of the 0-order and transferring that power into the scattered waves. Therefore, an aPSM offers both higher contrast and throughput than a traditional absorber for these critical patterns.[1] And yet it remains a challenge to precisely measure and control the relative phase shift of an EUV absorber, gating the introduction of EUV aPSMs.

We present a reflectometry-based metrology solution capable of achieving single picometer phase precision. The method requires measurements of absorber and multilayer reflectivity under varying illumination conditions. These measurements are then used in a multi-parameter nonlinear least-squares regression to determine a physical model for the multilayer and absorber. We validated our technique on a test mask which has a standard 40 bilayer Mo-Si multilayer mirror and a 60nm TaN absorber. To assess the empirical repeatability of the technique, we performed the reflectometry measurements multiple times for both multilayer and absorber. In the repeated measurements, we observed a systematic change in the absorber reflectivity not only during mask storage, but also during exposure itself.

We hypothesized that the most likely explanation would be a thin Carbon film growing on top of the absorber, because others have previously observed changes in the concentration of Carbon on Ta-based absorbers depending on storage conditions and EUV exposure.[2-4] Therefore, we assume all other layers remain constant and adjust only the Carbon layer when assessing repeatability of the technique. This yields

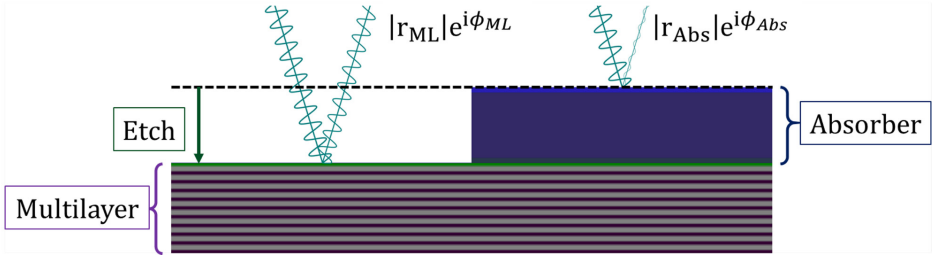

Figure 1. Photomask schematic depiction of reflections from absorber and multilayer. Absorber layers from top to bottom are: TaON-Ta-Ru-(Si-MoSi-Mo-MoSi)x40. Multilayer uses same film-stack, with an additional etch depth parameter to replace etched layers with vacuum. An additional C layer is added on top of the absorber, representing hydrocarbon contamination.

BACUS NEWS

FEBRUARY 2021
VOLUME 37, ISSUE 2

TAKE A LOOK INSIDE:

INDUSTRY BRIEFS
—see page 9

CALENDAR
For a list of meetings
—see page 10

SPIE.

11517-3

EDITORIAL

The Show ~~Must~~ Will Go On!

Set your calendars for upcoming mask conferences

Jed Rankin, GLOBALFOUNDRIES Inc. US

The one certainty in today's tumultuous world is that the effects of COVID-19 will continue to challenge all aspects of our business and drive flexibility and innovative solutions in our technology, communication, logistics, and planning. In 2020, we saw the cancellation of Photomask Japan (PMJ) in April, the postponement of the European Mask and Lithography Conference (EMLC) in June, and conversion of the September Photomask and EUV Lithography conference (BACUS/PUV) to an online digital forum.

While we are all getting a little too familiar with taking video calls from the kitchen, or seeing your boss's cat amble across his keyboard, the work associated with the demand for photomasks today and into the future continues. Like most business segments, the photomask industry has adopted new ways of working in the complex worldwide market. The changes are a mix of positive and negative, some of which should persist in the post-epidemic future, and some that could be abandoned.

The September 2020 Photomask and EUV Lithography conference reached record number of registrants by almost 3x compared to 2019 supported by online formats for presentations, discussions, and networking platforms. My experience was that the new medium allowed me to easily adjust conference participation to my schedule, review interesting topics, rewind a few seconds to understand complex issues, and engage with peers in ways I have not before. Although many worried about the challenges associated with the new format, most view it as an unprecedented success. There were obviously shortcomings, having primarily to do with the lack of face-to-face and impromptu discussions and networking

As we move into 2021, the impact of COVID-19 on this year's photomask conferences continues to be predictable only in its unpredictability. Currently, all three major Photomask conferences will be held, but each has adapted differently to the health and travel restrictions.

Photomask Japan (PMJ) has been changed to an all-digital forum on April 20 and 21st, from 8AM to 7PM JST. Digital content will be available for streaming during and after the conference for those who register. Additional details and updates are available at https://www.photomask-japan.org/

In a late-breaking update to the January 2021 BACUS newsletter's report, the 2021 European Mask and Lithography Conference (EMLC) has been converted to a novel panel-centric digital event on Tuesday, June 22nd 2021, covering Mask Manufacturing, EUV Lithography, Data analytics in Manufacturing, and Career Opportunities for university graduates in photomask and lithography industries. Additional Details and updates are available at https://www.emlc-conference.com/en. The program described in the January newsletter will be deferred to 2022. Careful readers of this newsletter may remember that the January 2021 editorial by Uwe Behringer described something quite different; while that form of EMLC is still planned, it will happen in 2022.

In September, the Photomask and EUV Lithography Conference (PUV) will be held September 26th-30th. It is too early to tell if we will all be together in Monterey, or if we'll attend from our living rooms in slippers, but the conference will go on. Please visit https://spie.org/conferences-and-exhibitions/photomask-technology--extreme-ultraviolet-lithography to find more details, or submit an abstract for this year's conference.

The COVID-19 global pandemic has changed business for all of us, but photomask manufacturing and development continue. Our key photomask conferences continue to be venues for learning, sharing ideas, and networking. So please, mark your calendars for these three great events, since the show must go on.

BACUS

N • E • W • S

BACUS News is published monthly by SPIE for *BACUS*, the international technical group of SPIE dedicated to the advancement of photomask technology.

Managing Editor/Graphics Linda DeLano
SPIE Sales Representative, Exhibitions, and Sponsorships Melissa Valum
BACUS Technical Group Manager Tim Lamkins

SPIE.

P.O. Box 10, Bellingham, WA 98227-0010 USA
Tel: +1 360 676 3290
Fax: +1 360 647 1445
SPIE.org
help@spie.org

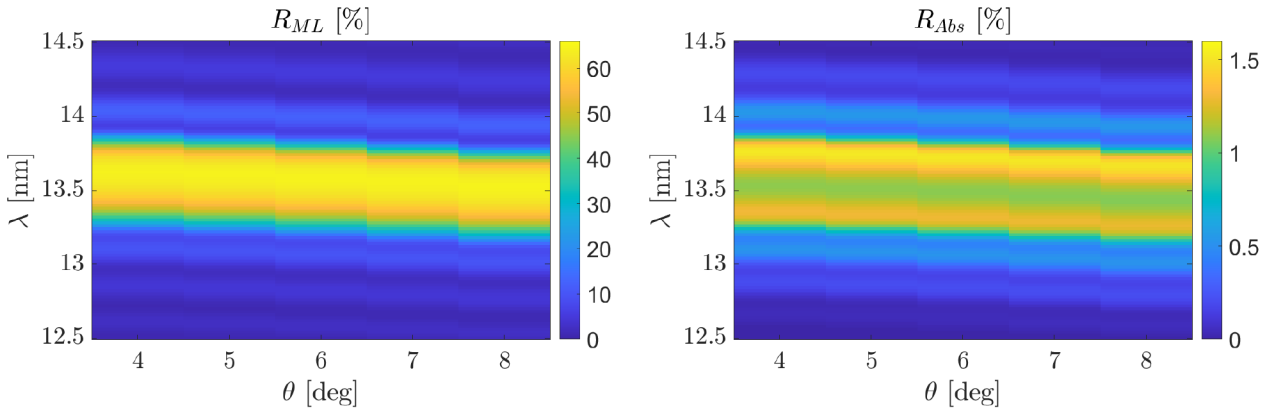

Figure 2. Reflectometry raw data scan of wavelength (y) and angle (x) for multilayer (left) and absorber (right). Note that the absorber reflectivity is not simply an attenuated multilayer reflection, and differs strikingly in that the absorber has a drop in reflectivity approximately where the multilayer attains its maximum value; this is due to destructive interference between the two primary components of the reflection coefficient.

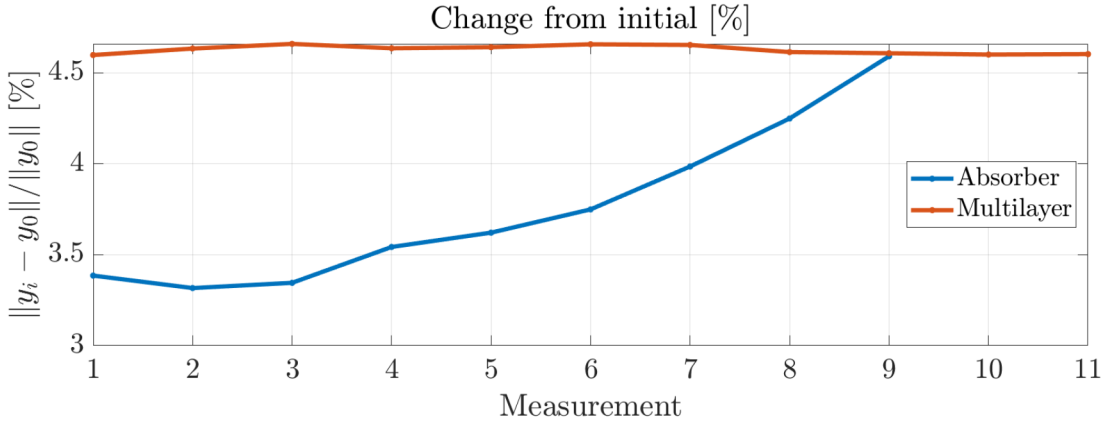

Figure 3. Changing reflectivity over time for multilayer and absorber. The multilayer experiences a 4.6% change as a result of storage between the initial measurement and the subsequent measurements (5 months), but then relatively little change over the remaining measurements. On the other hand for the absorber there is a relatively smaller 3.4% change after the first measurement (3 months), followed by a clear trend of increasing difference from the initial measurement, up to 4.6% by the final measurement.

a systematic trend of the Carbon thickness increasing monotonically from 44-156pm over the course of 10 reflectivity measurements of the absorber, causing a change in the phase of 0.3°. We estimate our precision to be 3σ = 0.1°.

Section 1 defines the mask geometry and experimental conditions. Section 2 defines the mathematical model and optimization approach. Section 3 shows the accuracy of our initial model, as well as the trend of Carbon growth. In section 4 we analyze the recovered phase to infer an effective propagation distance for absorber and multilayer; we also decompose the absorber signal into the interference of primary and secondary light paths to understand the impact of Carbon growth. Finally, in section 5 we quantify the precision of our method.

2. Experimental Methods

We characterize an EUV photomask using measurements of reflectivity from pure multilayer and absorber regions on the mask, taken at the Advanced Light Source Beamline 6.3.2. Figure 1 depicts a cross-sectional view of measuring multilayer and absorber reflectivity. Our reflectometer measures the amplitude-squared of the Fresnel reflection coefficient of each region; our goal is to extract the relative phase between these two reflections. The multilayer consists of a 2nm Ru cap as well as 40x MoSi bilayers; the "bilayers" actually contain 4 layers rather than 2 in our model, as an additional MoSi interdiffusion layer is added at both the Mo-Si and Si-Mo interfaces. The absorber has an additional 58nm TaN absorber topped with a 2nm TaON anti-reflection coating (ARC) layer; note that the ARC is to reject out-of-band DUV light and not to suppress the reflection of EUV. We further place a layer of pure Carbon on top of the TaON to represent contamination of the photomask absorber. The full table of fitted parameters is listed in the appendix.

We measure reflectivity for both multilayer and absorber over a range of wavelengths (12.5-14.5nm) and angles (4-8°), depicted in Figure 2. We are able to compress these two dimensions into a single k_z parameter for visualization purposes ($k_z = 2\pi \cos\theta/\lambda$) in Figure 4. This simplification is possible because over this measurement range the reflectance has very little dependence on the transverse wave vector because of planar symmetry. This implies the only variation between measurements at the same k_z but different angle would be due to variation in the refractive index over wavelength, which is relatively small over this range. We carried out our measurements multiple times to characterize precision. Ultimately we have an initial measurement for both multilayer and absorber, and an additional 11 multilayer and 9 absorber measurements. The latter 20 measurements were all collected back-to-back whereas the initial measurements were taken on earlier dates.

We choose to focus mostly on change over time only in the absorber

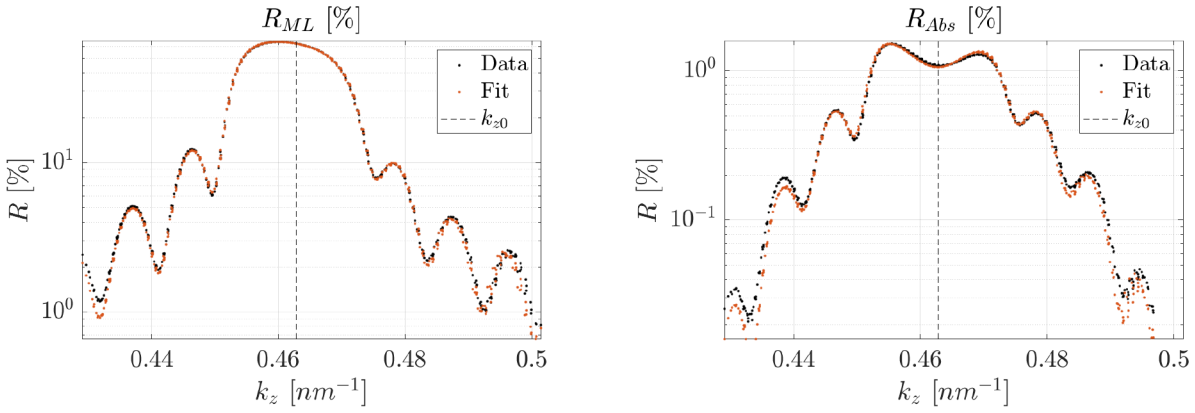

Figure 4. Modeled reflectivity vs k_z. Comparison of raw and fitted reflectivity based on initial 28 parameter fit, demonstrating the predictive power of our physical model.

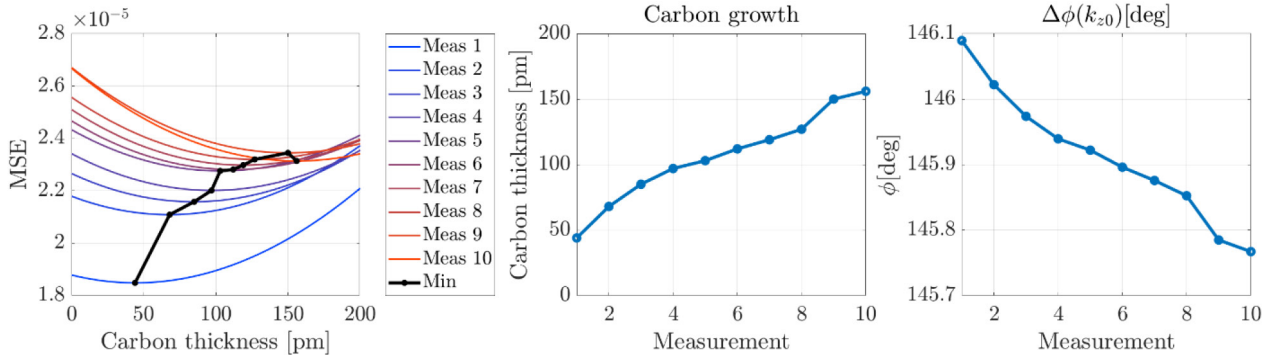

Figure 5. Carbon growth on absorber surface: single parameter fit to model contamination on absorber. Left MSE vs carbon thickness; black curve traces out optimal value for each absorber measurement. Center Recovered Carbon thickness, increasing from 44-156pm over 10 measurements. Right Relative phase between absorber and multilayer, decreasing from 146.1°-145.8°.

rather than the multilayer because of the relatively larger impact contamination on the absorber has for phase. Furthermore, we observe much more of a systematic trend in the absorber data changing over time. Figure 3 shows that there is a 4.6% relative change in the multilayer signal as a result of storage between the initial measurement and the subsequent measurements (5 months), but then relatively less change over the remaining measurements. The trend for the absorber on the other hand is quite different: there is a relatively smaller 3.4% change after the first measurement (3 months), followed by a clear trend of increasing difference from the initial measurement, up to 4.6% by the final measurement. This suggests that a measurable amount of contamination was likely growing on the surface of the absorber during the course of exposure itself. Hydrocarbon contamination is our hypothesis because it has been observed growing in both storage[2, 4] and during exposure,[2] as well as being cleaned during exposure in a scanner environment.[4] All this suggests that changes in the absorber are likely due to changes in a thin layer of organic contamination on top of the ARC. Growth of hydrocarbons by up to 0.9nm has been measured with AFM, although this method has an uncertainty of around 0.7nm,[2] so in this case it is hard to make a very quantitative statement. Nonetheless, this suggests that one or several monolayers of Carbon contamination could easily be induced by exposure during the reflectivity measurement.

3. Computational Methods

We parametrize each layer of our mask by a thickness and a concentration of each elemental species, and each interface is parametrized by its RMS surface roughness. Given all these physical parameters, we compute the Fresnel reflection coefficient[5] and compare its amplitude to a measurement of reflectivity vs wavelength and angle. We then perform an iterative optimization using cyclic coordinate descent with golden-section search, to find a set of physical parameters that most closely approximates the data for the initial measurement. We then freeze all but one parameter, the thickness of Carbon contamination on the absorber and perform a brute-force search, evaluating a range of thicknesses from 0-200pm and choosing the thickness with the lowest MSE.

4. Results

The results of the initial fit are shown in Figure 4, which demonstrates the predictive power of our physical model. Following this initial optimization, we freeze 27 of the 28 model parameters and perform a brute-force search for the Carbon contamination thickness. This is depicted in Figure 5. The left most plot shows the MSE vs Carbon thickness for the 10 absorber measurements; the black curve traces out the optimal value for each measurement. The recovered Carbon thickness is plotted in the center plot, increasing from 44-156pm over the course of the 10 measurements. The right most plot shows the resulting phase shift between the absorber and multilayer, which displays a total change of 0.3° from 146.1° – 145.8°. As to the question of how we could possibly be sensitive to thickness changes smaller than a single molecular monolayer, the answer is that we are measuring an average thickness across the area of the beam, and also including hundreds of measurements in our reconstruction. So the thickness reported is not necessarily uniform; in this way we can detect changes averaging only a fraction of a monolayer across the beam spot.

Table 1. Phase change across source for the 0.33 and 0.55 NA systems, based on recovered $\vartheta\phi_{rel}/\vartheta k_z$ = 48nm. For both systems a 2% λ variation leads a to 25.5° variation in the phase. The 0.33 NA system also has substantial variation in the Y direction (22.1°) but much less in X (4.4°). In contrast, in the 0.55 NA system the variation is reduced in Y (16.6°) but greatly increased in X (12.2°).

NA	$\Delta\phi_\lambda$ [2%]	$\Delta\phi_{\theta_y}$	$\Delta\phi_{\theta_x}$	m_y	m_x	θ_0	θ_y^{max}	θ_x^{max}
0.33	25.5°	22.1°	4.4°	4	4	6.0°	10.7°	7.7°
0.55	25.5°	16.4°	12.2°	8	4	5.355°	9.3°	9.6°

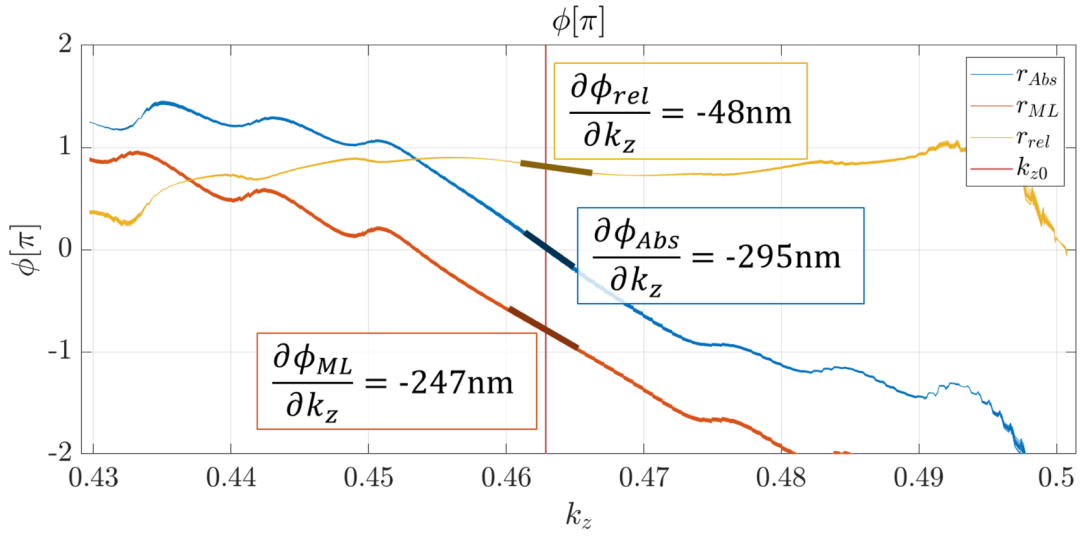

Figure 6. Recovered phase based on fitted Fresnel reflection coefficient from initial 28 parameter fit for absorber (blue), multilayer (red), and relative (yellow). The phase gradient $\vartheta\phi/\vartheta k_z$ represents an effective propagation distance. The absorber has a significantly larger effective propagation distance than the multilayer (295nm vs 247nm), which will impact the Mask 3D (M3D) effects. Additionally, the resulting 48nm difference in propagation distance will cause variation in the pattern phase vs the illumination condition.

5. Analysis

From our initial model, we can extract the phase as a function of k_z, shown in Figure 6. In addition to the relative phase shift between mulitilayer and absorber at the nominal operating condition $k_{z0} = 2\pi \cos 6°/(13.5\text{nm})$, we can also use our model to obtain useful information about mask 3D effects from the gradient $\vartheta\phi=\vartheta k_z$. This gradient represents an effective propagation distance for each reflection coefficient. The propagation distance for the multilayer is 247nm, including both reflection by the multilayer and transmission twice through vacuum of equal height to the absorber. The propagation distance for the absorber on the other hand increases by 48nm (19%), to 295nm. These propagation distances will directly scale pattern translation vs angle meaning that for this mask light reflected from the absorber will translate 19% further than light reflected from the multilayer, impacting M3D effects and how they scale with pitch. Additionally, this will result in different phase for source points with different k_z. Difference in k_z could arise from variation in either angle or wavelength. For this mask a 2% change in wavelength would cause a phase shift of $\Delta\phi_\lambda = (\vartheta\phi/\vartheta k_z)\, k_0\, (2\%) = 25.5°$. A change in angle from one edge of the pupil to the other (Y, shadowing orientation) would cause a phase shift of $\Delta\phi\theta_y = (\vartheta\phi/\vartheta k_z)\, k_0\, [\cos\theta_{min} - \cos\theta_{max}] = 22.1°$ and 16.4° for the 0.33 and 0.55 NA systems respectively; the effect is somewhat mitigated in the higher NA system due to the increased magnification and decreased chief-ray angle. On the other hand we observe the opposite trend in the X direction due to increased mask-side NA, where the variation increases from 4.4° to 12.2°. These effects are summarized in Table 1. Therefore, it would seem that the changing phase shift across the source may be a key factor in designing future EUV aPSMs.

It is not immediately obvious why the propagation distance for the absorber would be so much larger than the multilayer; after all, Ta is supposed to have a refractive index less than 1 at this wavelength meaning that if anything we would expect a shorter effective propagation distance compared to vacuum. However, the story is made somewhat more complicated by the fact that the absorber reflection is approximately the interference between two reflections: the primary and much stronger reflection is light that transmits twice through the absorber and is reflected by the multilayer, whereas the secondary and relatively weaker reflection is light that is reflected by the absorber without interacting with the multilayer.

This interference process is illustrated in Figure 7, where we decompose the total reflection (blue) into its primary (red) and secondary (yellow) components. We display this decomposition for the initial and final measurements, as well as the difference from initial to final (top to bottom). We can see that for both the initial and final measurements, the primary and secondary reflections are almost exactly out of phase at k_{z0}, causing destructive interference and hence a dip in reflectivity. The difference shows clearly that the left peak shrinks while the right peak grows as the location of maximum destructive interference shifts slightly.

6. Precision

We can consider computing precision in two ways. If we assume no physical change in the photomask over the course of measurements, we would compute the precision from the standard deviation of the measured phase, yielding $3\sigma = 0.9°$. However, since we have observed monotonic thickness and phase change, it seems more physically plausible that the changes in the signal are largely real and the uncertainty should only be whatever remaining variation cannot be accounted for physically. To approximate this uncertainty, we compute the standard deviation of the residuals of a linear fit, where the linear component now represents physically real changes and the residuals represent random uncertainty. This method yields $3\sigma = 0.15°$, suggesting that the vast majority of the

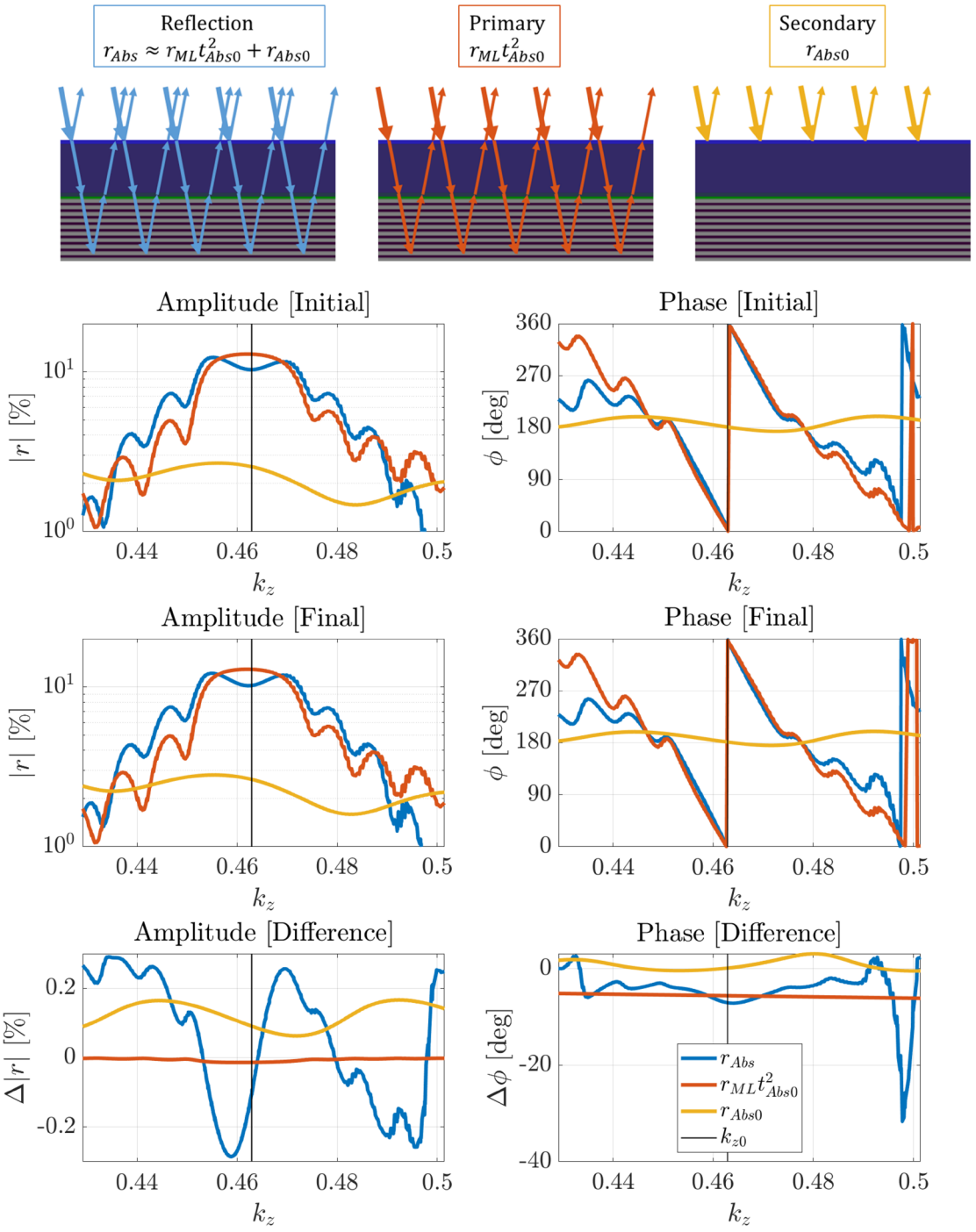

Figure 7. Schematic illustration of decomposing absorber reflection into primary and secondary components. Initial measurement: *The amplitude of the primary component closely follows the amplitude of the multilayer reflection coefficient, whereas the amplitude of the secondary component has additional features, such as the local minimum at* k_{z0}. Final measurement: *After the growth of approximately 100pm of Carbon, a slight lateral motion of the central local minimum is observed.* Difference: *We can much more easily observe the changes due to Carbon growth from the difference of the final minus initial model. We observe the left peak decreasing and the right peak increasing by a similar amount.*

signal variance is explicable by a linear drift, as can be seen qualitatively in Figure 5. If we exclude the first point because it was collected on a separate date, our precision would improve to 0.11°. If we were to further remove the final two points where there is a noticeable deviation from the trend, the precision would further improve to 0.08°. So we estimate the precision to be approximately 3σ = 0.1°, a value consistent with the latter two methods.

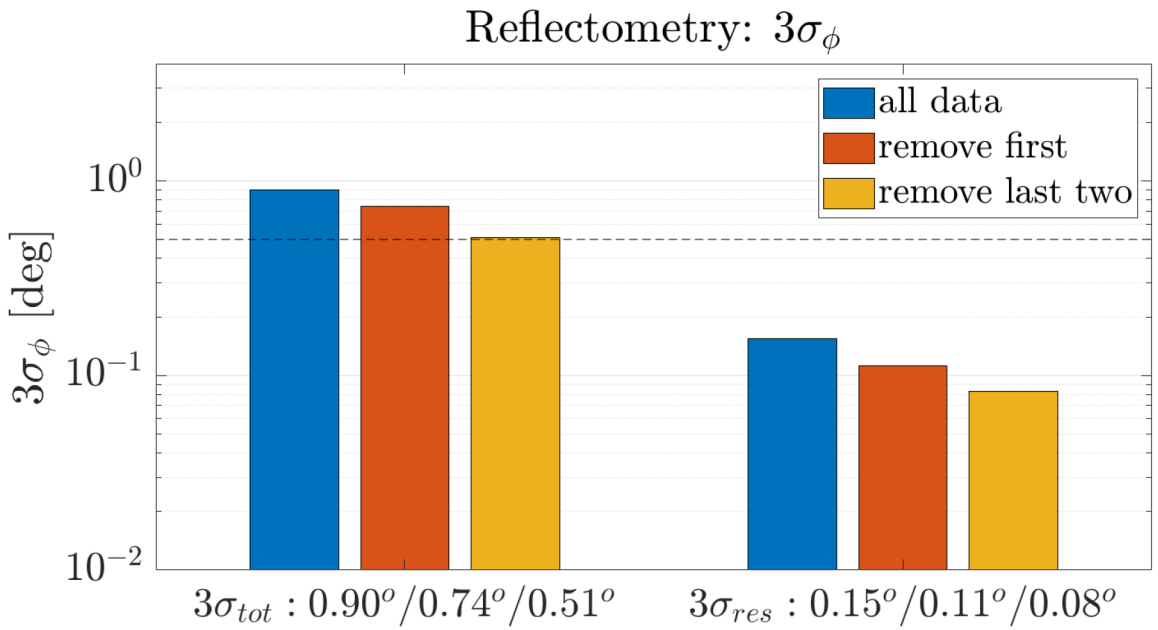

Figure 8. Precision 3σ of total and linear residuals. Because we believe the drift in the signal is physically real, linear residuals give a better approximation of the precision. In all three cases the vast majority of the variance in the data is explained by the linear trend due to the systematic trend in Carbon thickness and phase. Blue shows the statistics including all data points; red includes all but the first point (collected on a different date); and yellow further removes the final two points, which show a noticeable deviation from the linear trend. Note that all three methods give fairly similar precision statistics, the latter two yielding approximately 3σ = 0.1°

7. Conclusion

We have presented a computational reflectometry technique to characterize the phase of an EUV photomask via measurements of reflectivity from multilayer and absorber regions. A 28 parameter physical model was capable of producing a highly accurate match to the experimental reflectivity data. We use the physical model to extract the relative phase of the absorber and multilayer reflections, as well as the phase gradient with respect to k_z, which represents an effective propagation distance for each reflection coefficient. According to our model, the effective propagation of the absorber is 295nm, which is 48nm further than the propagation of the multilayer (247nm). It appears that the source of the increased propagation distance is destructive interference between a primary component which is reflected by the multilayer and twice transmitted through the absorber, and a much weaker secondary component which is reflected purely by the absorber. We also find that the absorber reflectivity changes systematically from one measurement to the next, unlike the multilayer which displayed changes during storage, but not during exposure. We attributed the changes in absorber reflectivity to hydrocarbon contamination, which we believe is the most plausible explanation. In a subsequent single-parameter fit, we determined that the Carbon layer grew from an estimated 44-156pm over the course of 10 exposures, causing a change in the phase shift of approximately 0.3°; although these changes amount to only a fraction of an atomic monolayer, we can measure the average thickness across the beam-spot to sub-atomic precision. Based on the deviation of our recovered phase from a linear trend, we estimate that our measurements have a precision of 3σ = 0.1° or 3-4pm in terms of the 13.5nm wavelength.

8. Acknowledgments

This research is sponsored by C-DEN (Center for Design-Enable Nanofabrication). Member companies – ARM, ASML, Cadence, Carl Zeiss Group, Intel, KLA-Tencor, Mentor Graphics, and Qualcomm.

This work was performed in part at Lawrence Berkeley National Laboratory which is operated under the auspices of the Director, Office of Science, of the U.S. Department of Energy under Contract No. DE-AC02-05CH11231.

9. References

[1] M. -C. van Lare, F. J. Timmermans, and J. Finders, "Alternative reticles for low-k1 euv imaging," in *International Conference on Extreme Ultraviolet Lithography 2019,* **11147**, p. 111470D, International Society for Optics and Photonics, 2019.

[2] C. -C. Wu, M. Bender, R. Jonckheere, F. Scholze, H. Bekman, M. van Putten, R. de Zanger, R. Ebeling, J. Westerhout, K. Nicolai, *et al.*, "Lifetime test on euv photomask with ebl2," in *Photomask Japan 2019: XXVI Symposium on Photomask and Next-Generation Lithography Mask Technology,* **11178**, p. 111780E, International Society for Optics and Photonics, 2019.

[3] S. Singh, B. Yatzor, R. Taylor, O. Wood, and P. Mangat, "A study on euv reticle surface molecular contamination under different storage conditions in a hvm foundry fab," in *Extreme Ultraviolet (EUV) Lithography VIII,* **10143**, p. 101431T, International Society for Optics and Photonics, 2017.

[4] R. Jonckheere, V. V. Nair, E. Hendrickx, R. Aubert, C. -C. Wu, V. de Rooij-Lohmann, D. Elstgeest, H. Lensen, V. Soltwisch, P. Hoenicke, *et al.*, "Study of euv reticle storage effects through exposure on ebl2 and nxe," in *Extreme Ultraviolet Lithography 2020,* **11517**, p. 115170Z, International Society for Optics and Photonics, 2020.

[5] S. Sherwin, I. Cordova, R. Miyakawa, L. Waller, A. Neureuther, and P. Naulleau, "Quantitative phase retrieval for euv photomasks," in *Extreme Ultraviolet (EUV) Lithography XI,* **11323**, p. 1132315, International Society for Optics and Photonics, 2020.

[6] S. Sherwin, I. Cordova, L. Waller, A. Neureuther, and P. Naulleau, "Measuring the phase of euv photomasks," in *International Conference on Extreme Ultraviolet Lithography 2019,* **11147**, p. 111471F, International Society for Optics and Photonics, 2019.

10. Appendix

6.1 Table of parameters

Complete fit result for all 28 parameters that were allowed to vary in the initial 28 parameter fit. Notes on modeling: Layers listed from top to bottom. Roughness is RMS roughness of the interface above the listed surface. Concentration is as a percentage of a nominal concentration; n and k are calculated using a weighted sum of delta and beta from CXRO database, as described in.[6] "Etch thick" is the un-etched thickness on the multilayer, starting from the Ru capping layer. If it is equal to the Ru thickness, then the etch perfectly stops at the Ru; a value lower than the Ru thickness implies the Ru layer been partially etched; while a value higher (as we have in the fit) implies an incomplete etch (in this fit, about 3.17-2.32=0.85nm TaN remains on top of the Ru cap in the multilayer region).

	Lower Bound	Nominal	Fit	Upper Bound
Thickness [nm] C	0.00	0.00	0.00	0.50
Thickness [nm] TaON	0.00	2.00	2.69	4.00
Thickness [nm] TaN	55.00	58.00	58.92	61.00
Thickness [nm] Ru	1.50	2.00	2.32	2.50
Thickness [nm] Si	3.16	3.24	3.26	3.32
Thickness [nm] Mo	2.11	2.16	2.17	2.21
Roughness [nm] C	0.00	0.00	0.09	1.00
Roughness [nm] TaON	0.00	0.00	0.01	1.00
Roughness [nm] TaN	0.00	0.00	0.24	1.00
Roughness [nm] Ru	0.00	0.00	0.00	1.00
Roughness [nm] Si	0.00	0.00	0.04	0.20
Roughness [nm] MoSi2	0.00	0.00	0.01	0.20
Roughness [nm] Mo	0.00	0.00	0.00	0.20
Roughness [nm] MoSi2	0.00	0.00	0.01	0.20
Concentration [%] C - C	0	100	77	300
Concentration [%] TaON - Ta	0	33	54	300
Concentration [%] TaON - N	0	33	197	20000
Concentration [%] TaON - O	0	33	449	20000
Concentration [%] TaN - Ta	0	50	58	300
Concentration [%] TaN - N	0	50	0	20000
Concentration [%] Ru - Ru	0	100	35	300
Concentration [%] Si - Si	0	100	89	300
Concentration [%] MoSi2 - Si	67	67	51	300
Concentration [%] MoSi2 - Mo	33	33	29	200
Concentration [%] Mo - Mo	0	100	64	200
Concentration [%] MoSi2 - Si	67	67	133	300
Concentration [%] MoSi2 - Mo	33	33	30	200
Etch thick [nm]	1.0	2.0	3.2	4.0

Industry Briefs

Micron Pulls Ahead on DRAM

By Gary Hilson, EETimes

Micron Technology has unveiled its 1-alpha node DRAM, which the company said offers a 40% improvement in memory density over its 1z node DRAM, as well as a 15% improvement in power-savings for mobile devices. This latest memory node supports densities from 8Gb to 16Gb, and Micron has started volume production of DDR4 memory for compute customers and Crucial consumer PC DRAM products on the new process node, while LPDDR4 is being sampled to mobile customers for qualification.

https://www.eetimes.com/micron-pulls-ahead-on-dram/

Major Taiwan Chipmakers to Assign Capacity for Car Use

Focus Taiwan, CNA English News

Taipei, Jan. 27 (CNA) Four major contract chipmakers in Taiwan have agreed to assign capacity to manufacture chips for car use in a bid to alleviate a global shortage of automotive chips, Minister of Economic Affairs Wang Mei-hua (王美花) said, after she met with representatives from the four contract chipmakers — Taiwan Semiconductor Manufacturing Co. (TSMC), United Microelectronics Corp. (UMC), Vanguard International Semiconductor Co. (VIS) and Powerchip Technology Corp. — at a time when global automakers have urged Taiwan to increase automotive chip supplies.

In 2019, automakers cut their orders for chips, prompting local chipmakers to shift their capacity to producing chips for other devices, according to Wang. After the outbreak of the COVID-19 pandemic, demand for notebook computers, smartphones and other devices in a booming global stay-at-home economy further squeezed more of the capacity previously used for car chips. Currently, capacity of the four companies has been almost fully utilized. The urging by global automakers to Taiwan's semiconductor industry for an increase in chip supply indicates that Taiwan plays a key role in the world's economy, the minister said.

The current chip shortage has prompted TSMC and other Taiwanese chipmakers to consider a 15 percent hike in their automotive chip prices which could start in late February.

https://focustaiwan.tw/business/202101270021

China Surges Past Americas and Japan in IC Capacity

Christian G. Dieseldorff, SEMI

Back in 2012, China ranked fifth among seven regions worldwide in IC wafer capacity but surged past the Americas and Japan in 2018 and 2019 to claim the number three position. China's IC wafer capacity growth accelerated to the tune of 14% in 2019 and 21% in 2020 and is expected to grow at least 17% this year. But Chinese companies aren't pulling off this feat single-handedly. Among international-owned companies, TSMC and UMC are driving the largest share of foundry growth, while Samsung, SK Hynix and Intel are powering gains in memory capacity.

https://blog.semi.org/business-markets/china-surges-past-the-americas-and-japan-in-ic-capacity

Join the premier professional organization for mask makers and mask users!

About the BACUS Group

Founded in 1980 by a group of chrome blank users wanting a single voice to interact with suppliers, BACUS has grown to become the largest and most widely known forum for the exchange of technical information of interest to photomask and reticle makers. BACUS joined SPIE in January of 1991 to expand the exchange of information with mask makers around the world.

The group sponsors an informative monthly meeting and newsletter, BACUS News. The BACUS annual Photomask Technology Symposium covers photomask technology, photomask processes, lithography, materials and resists, phase shift masks, inspection and repair, metrology, and quality and manufacturing management.

Individual Membership Benefits include:

- Subscription to BACUS News (monthly)
- Eligibility to hold office on BACUS Steering Committee

spie.org/bacushome

Corporate Membership Benefits include:

- 3-10 Voting Members in the SPIE General Membership, depending on tier level
- Subscription to BACUS News (monthly)
- One online SPIE Journal Subscription
- Listed as a Corporate Member in the BACUS Monthly Newsletter

spie.org/bacushome

CALENDAR

2021

SPIE Advanced Lithography
22-26 February 2021
Digital Forum
www.spie.org/al

Photomask Japan
20-21 April 2021
Digital Forum
Japan
www.photomask-japan.org

The 36th European Mask and Lithography Conference, EMLC 2021
22 June 2021
Digital Event
www.emlc-conference.com/en

SPIE Photomask Technology + EUV Lithography
26-30 September 2021
www.spie.org/conferences-and-exhibitions/photomask-technology--extreme-ultraviolet-lithography

SPIE is the international society for optics and photonics, an educational not-for-profit organization founded in 1955 to advance light-based science and technology. The Society serves more than 255,000 constituents from 183 countries, offering conferences and their published proceedings, continuing education, books, journals, and the SPIE Digital Library in support of interdisciplinary information exchange, professional networking, and patent precedent. In 2019, SPIE provided more than $5 million in community support including scholarships and awards, outreach and advocacy programs, travel grants, public policy, and educational resources. **spie.org**

SPIE.
International Headquarters
P.O. Box 10, Bellingham, WA 98227-0010 USA
Tel: +1 360 676 3290
Fax: +1 360 647 1445
help@spie.org • **spie.org**

Shipping Address
1000 20th St., Bellingham, WA 98225-6705 USA

Managed by SPIE Europe
2 Alexandra Gate, Ffordd Pengam, Cardiff,
CF24 2SA, UK
Tel: +44 29 2089 4747
Fax: +44 29 2089 4750
spieeurope@spieeurope.org • **spieeurope.org**

You are invited to submit events of interest for this calendar. Please send to lindad@spie.org.